Distance Dependence of the Interaction between Single Atoms: Gold Dimers on NiAl(110)

N. Nilius, T. M. Wallis,* M. Persson,† and W. Ho‡

Department of Physics and Astronomy and Department of Chemistry, University of California, Irvine, California 92697-4575, USA

(Received 8 August 2002; published 14 May 2003)

The importance of substrate-mediated adsorbate-adsorbate interactions on electronic states has been demonstrated for Au dimers on NiAl(110) with a scanning tunneling microscope and density functional calculations. An unoccupied resonance observed in single Au atoms splits into a doublet in Au dimers. The energy splitting depends inversely on the distance between the two adatoms, revealing the relative importance of direct and substrate-mediated interactions. Spatially resolved conductance measurements of Au dimers reveal the symmetric and antisymmetric characters of the doublet states.

DOI: 10.1103/PhysRevLett.90.196103 PACS numbers: 68.37.Ef, 73.20.–r, 73.22.Dj, 73.43.Cd

The electronic properties of adatoms on surfaces are determined not only by their coupling to the substrate but also by adatom-adatom interactions. The coupling between adsorbate electronic states plays a crucial role in various phenomena on surfaces, such as adsorption, nucleation, and chemistry [1]. In its most elementary form, the interaction occurs between two identical atoms forming a dimer. Because of their simple structure, dimers are extremely attractive for both experiment and theory to study coupled electronic states [2–7].

Adsorption stabilizes the adatoms on sites of the underlying lattice, thus enabling atom-atom distances different from the corresponding gas phase dimers. Electronic interactions between adatoms involve direct coupling between adatom orbitals and indirect coupling through substrate electronic states. Direct interactions, responsible for the bonding in free dimers, are characterized by the formation of bonding and antibonding states. The resulting level splitting decays exponentially with the separation between the dimer atoms. Direct coupling mechanisms have been thoroughly investigated on metal dimers in the gas phase and noble-gas matrices [7–9]. Indirect coupling through substrate states was primarily investigated for its effects on the adatom-adatom interaction energy, but not on adatom electronic states [3,10]. The interaction energy depends sensitively on the electronic structure of the support and follows different power laws as a function of distance. Indirect coupling often gives rise to long-ranged interactions between adatoms and plays a crucial role for nucleation and growth processes on surfaces [2,11–14].

Experiments on the influence of direct and indirect interactions on the electronic states of adatoms require a local spectroscopic technique, which is sensitive to individual atoms. In this Letter, scanning tunneling microscopy (STM) and scanning tunneling spectroscopy (STS) were combined to obtain structural as well as local electronic characterization of adatoms. The experiments show how a single resonance in Au atoms on NiAl(110) splits into a symmetric and an antisymmetric state in Au dimers. The underlying interaction mechanisms between the adatoms and the role of the substrate were identified with density functional theory (DFT).

The experiments were carried out in an ultrahigh vacuum STM operated at 12 K [15]. The NiAl(110) surface was prepared by cycles of Ne^+ sputtering and annealing to 1300 K. The alloy surface consists of alternating rows of Ni and Al atoms with a periodicity of 4.1 Å. Atoms along the rows are separated by 2.9 Å. Gold was evaporated from an alumina crucible and deposited on the surface at 12 K. From STM topographic images, the preferential Au binding site was identified as the bridge position on the Ni rows [Fig. 1(a)]. Approximately 10% of the atoms coalesce to aggregates of two and three atoms in varying configurations. Gold dimers appear as elongated structures; the positions of the dimer atoms are not resolved due to the strong overlap of their atomic wave functions. The adsorption geometry was, however, determined from the angle between dimer axis and Ni rows.

Four different dimer configurations were identified on NiAl(110), designated as types I–IV in the following text. Type I is oriented along the Ni rows and shows the smallest spacing between the Au atoms. The atoms are adsorbed on adjacent bridge sites of the same Ni row, separated by 2.9 Å [Fig. 1(b)]. The axis of dimer II is oriented perpendicular to the Ni rows and the Au pair sits in neighboring sites on two Ni rows, leading to a bond length of 4.1 Å [Fig. 1(c)]. Dimer III is tilted by $\pm 54.7°$ with respect to the Ni rows. The two atoms occupy second nearest neighbor sites on adjacent Ni rows and are 5.1 Å apart [Fig. 1(d)]. Dimer IV is formed by two atoms in second nearest neighbor positions of the same Ni row, separated by 5.8 Å [Fig. 1(e)]. The existence of two equivalent orientations favors the formation of dimer III, which was more frequently found in the experiments than dimers I, II, and IV.

The different bond lengths of Au dimers on NiAl(110) allow an investigation of the distance dependence of their interactions. Electronic properties were probed by STS, which detects the first derivative of the tunneling current as a function of sample bias (dI/dV) and gives a measure

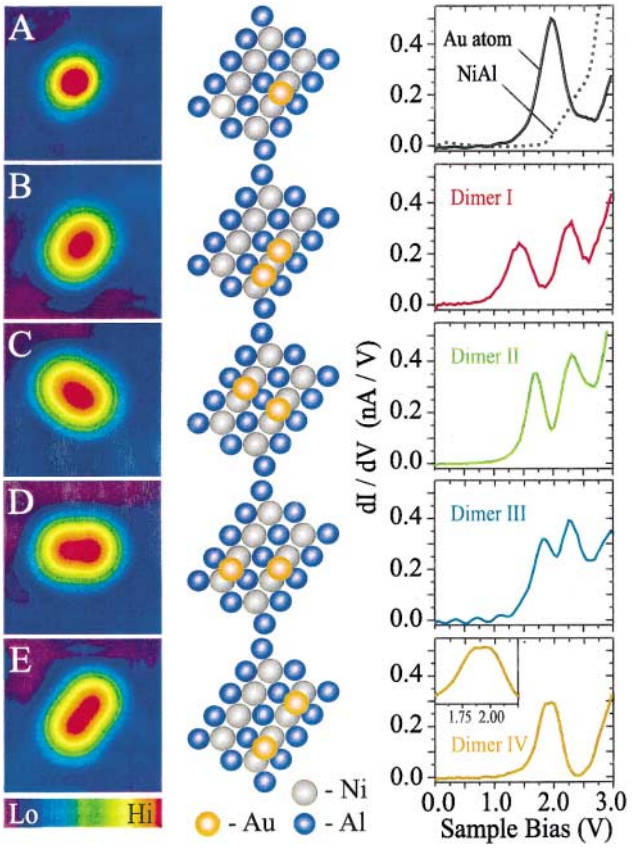

FIG. 1 (color). (a)–(e) Topographic images (size 25 Å × 25 Å, $V_{\text{sample}} = 2.0$ V, $I = 0.1$ nA), structure models, and dI/dV spectra for a Au atom and different Au dimers on NiAl(110). The tunnel gap for dI/dV spectra was set with $V_{\text{sample}} = 2.0$ V, $I = 0.1$ nA.

of the local density of states (LDOS) of the sample. Conductance measurements on top of a Au atom reveal a Gaussian shaped resonance in the empty DOS at +1.95 V [Fig. 1(a)]. The dI/dV peak vanishes for tip positions slightly off the atom, where a smoothly increasing NiAl signal is detected. The conductance at negative bias is similar for Au atoms and the bare surface. Positioning the tip above the center of a dimer leads to a distinct splitting of the 1.95 V resonance (Fig. 1). Both peaks in the doublet are almost evenly displaced relative to the single-atom resonance. The largest splitting of 0.8 V is observed for dimer I with peak positions at 1.5 and 2.3 V. Conductance peaks at 1.7 and 2.3 V emerge in the spectra of the perpendicular dimer II, leading to a splitting of 0.6 V. The energy separation decreases further to 0.4 V in dimer III, with peaks around 1.8 and 2.2 V. For the biggest atom-atom distance in dimer IV, the doublet collapses to two overlapping peaks at 1.85 and 2.05 V. For Au pairs with larger spacing, both atoms show the 1.95 V resonance of an isolated atom. The peak splitting in Au dimers as a function of interatomic separation is summarized in Fig. 2. The points result from averaging over 200 different dimers; the error bars indicate the variations in the observed peak splittings.

To analyze the interrelation between bond length and peak splitting in Au dimers and the role of the NiAl substrate, we have carried out DFT calculations using a plane wave and the projector augmented wave method. The calculations were based on the VASP code and the PW91 version of generalized gradient approximation for the exchange and correlation effects [16]. The system was represented by a dilute ordered overlayer of Au atoms and dimers on a slab of eight NiAl layers [17]. The Au bonding geometry on Ni bridge sites was obtained by structural optimization. The dI/dV spectra were simulated by the Tersoff-Hamann approach for tunneling in a STM junction, using an s-wave approximation for the tip [18]. The dI/dV signal is here proportional to the LDOS at the tip apex, obtained from Kohn-Sham states of the sample calculated in the absence of the tip [19]. The introduction of an external electric field in the self-consistent cycles of the calculation simulates the tip-induced Stark shift on sample states [20]. Calculations for the bare NiAl(110) surface reveal a depletion zone in the LDOS between 1.0 and 2.5 eV above the Fermi level, resulting from gaps in the projected bulk band structure in parts of the Brillouin zone [21]. The upper edge of this pseudogap is reflected in a sudden onset in the LDOS around 2.5 V [Fig. 3(a)], also observed in dI/dV spectra of the bare surface [Fig. 1(a)]. In this pseudogap, the Au adatom induces a resonance state with sp character, which originates from the hybridization of Au 6s, p and NiAl states [Fig. 3(b)]. The 6s and 6p states in isolated Au atoms are located at −1.2 and 3.9 eV. Because of interactions with the substrate, the 6s state induces two resonance states split by 5 eV, while the 6p state shifts down in energy and becomes a broad resonance with considerable 6s intermixing [Fig. 3(b)].

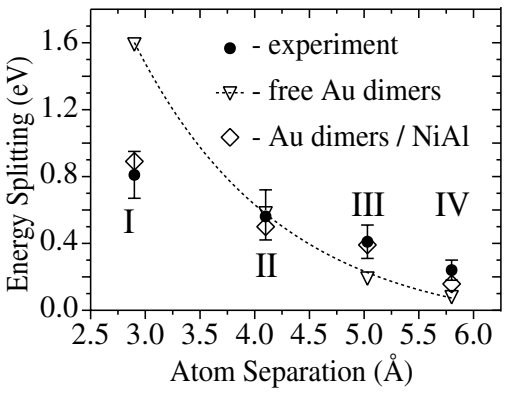

FIG. 2. Experimental energy splitting (●) of resonances in Au dimers I–IV on NiAl(110) as a function of interatomic distance. Error bars reflect the distribution in energy splitting obtained from 200 dimers. Calculated splittings for free (▽) and NiAl-supported Au dimers (◇) are shown for comparison. The dashed line is an exponential fit through the calculated splittings in free dimers.

In the absence of an external electric field, the state appears as a peak at +1.75 V in the LDOS calculated at the position of the tip [Fig. 3(b)]. Because of the Stark effect induced by a tip electric field of 0.25 V/Å, the peak shifts to +1.91 V in agreement with the experimental value of +1.95 V [22]. Mixed states with mainly Au 5*d* and Ni 3*d* character are more localized at the Au atom and do not contribute to the LDOS at the tip apex.

In dimers on NiAl(110), the single-atom resonances interact and form a symmetric and an antisymmetric state. The resonance splitting is illustrated by the calculated LDOS for dimer I, exhibiting two peaks at 1.2 and 2.1 V [Fig. 3(c)]. The Stark effect changes the calculated peak separation by less than 0.05 eV. The low-energy peak shows a maximum in the LDOS between the two atoms, reflecting its symmetric character [Fig. 3(d)]. The high-energy peak has a nodal plane, consistent with an antisymmetric state [Fig. 3(e)]. For the other dimer configurations, similar states with symmetric and antisymmetric character were obtained. The calculated peak separations for the Au dimers I–IV on NiAl(110) reproduce the experimental results (Fig. 2).

To gain a better understanding of the substrate influence on the electronic interactions between Au atoms, the electronic properties of free Au dimers were calculated using identical interatomic distances as for the dimers I–IV. The interaction in free dimers is induced by a direct overlap of the Au 6*s* orbitals and leads to substantial splitting into a bonding and an antibonding level for small bond lengths (Fig. 2). The level separation decays exponentially with increasing interatomic distance *d*, in contrast to the slowly diminishing resonance splitting Δ_{aa} observed in the experiment. The difference emphasizes the importance of substrate electronic properties in determining Δ_{aa}. For small *d* (dimer I), the substrate "screens" direct orbital interactions, because the strong hybridization of the Au 6*s, p* orbitals with NiAl states reduces the effect of directly overlapping Au orbitals. For larger *d* (dimer IV), the coupling is mainly mediated by substrate electronic states and leads to measurable Δ_{aa} far beyond the influence of the 6*s, p* overlap. Electrons propagating through substrate electronic states result in a different *d* dependence of Δ_{aa} than direct orbital overlap. For instance, the amplitude decay of electrons propagating in free space leads to a $1/d$ dependence in Δ_{aa} for two *s*-resonance scatterers [23]. In the case of surface-state mediated coupling, corresponding to a 2D propagation of electrons, Δ_{aa} should decay as $1/\sqrt{d}$, in contrast to the observed $1/d$ dependence.

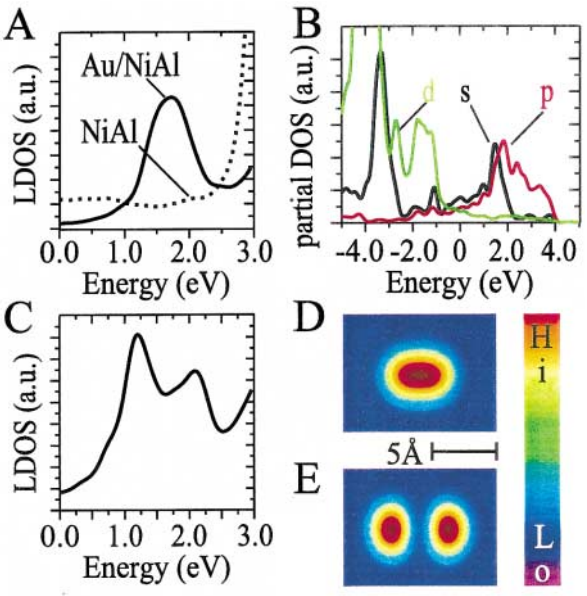

FIG. 3 (color). (a) Calculated LDOS for a single Au atom on NiAl(110) (solid line) and the bare surface (dashed line). (b) Partial wave decomposition of the DOS for the Au atom. (c) LDOS above one atom in Au dimer I. (d) LDOS contour plot of dimer I calculated at 1.2 V and (e) 2.1 V, showing the symmetric and antisymmetric character of the corresponding resonances. The LDOS was calculated for a constant height of 6 Å above the NiAl plane, which leads to a smaller size of the dimer than in experimental constant current images.

The symmetric and antisymmetric character of the two resonances in Au dimers on NiAl(110) was directly observed by spatially resolved dI/dV measurements, taking spectra at different tip positions along the dimers axis. For the close-spaced dimer I, the spectra reveal the characteristic peak splitting of 0.8 V [Fig. 4(a)]. The low-energy resonance at 1.5 V emerges at all positions along the dimer axis but exhibits an intensity maximum in the center. The peak at 2.3 V shows the highest intensity on both ends of the dimer and a diminishing signal between the atoms. A similar spatial distribution was derived from dI/dV microscopic images, which simultaneously detect topographic and dI/dV information at a fixed bias. For dimer I, the low-energy resonance at 1.5 V is delocalized over the whole structure [Fig. 4(b)]. At 2.3 V sample bias, the dI/dV signal for the Au dimer is lower than that of the surrounding NiAl surface [Fig. 4(b)]. The conductance at 2.3 V shows a prominent minimum between the atoms and enhanced intensity at both ends of the dimer. The variations in conductance at 1.5 and 2.3 V are illustrated by cuts through dI/dV microscopic images and follow the dI/dV signal obtained from spatially resolved spectroscopic measurements [Fig. 4(c)]. The spatial distribution of the low-energy resonance matches the calculated symmetric character of the corresponding state [Fig. 3(d)]. The presence of a nodal plane reflects the antisymmetric character of the high-energy resonance. Conductance resonances with symmetric and antisymmetric character were also observed for the Au dimers II and IV. In all three configurations, the dimer axis follows major crystallographic directions of NiAl(110), leading to the expected symmetry of the electronic states. The resonances of dimer III show a different spatial

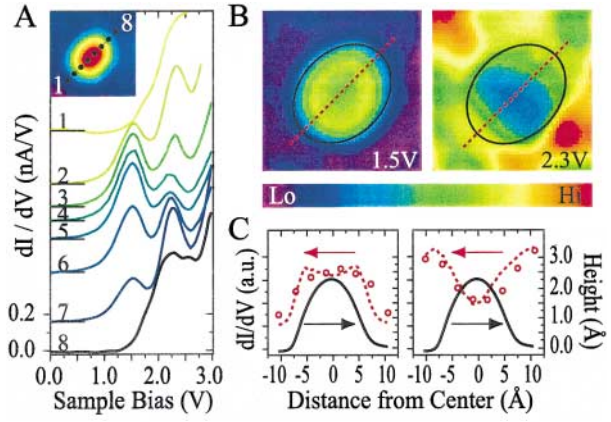

FIG. 4 (color). (a) dI/dV spectra for Au dimer I, measured at different points along the dimer axis as shown in the inset. The tunnel gap was set with $V_{\text{sample}} = 2.0$ V, $I = 0.1$ nA. (b) dI/dV microscopy images of dimer I (size 26 Å $\times$ 26 Å), taken at the positions of the low- (left) and the high-energy (right) resonance. (c) Cross sections through dI/dV images from (b) (broken lines) and corresponding dI/dV intensities at 1.5 and 2.3 V from spectra shown in (a) (circles). The topographic heights of dimer I above the NiAl surface are included for comparison (solid lines).

distribution, most likely due to the tilted adsorption geometry of the dimer with respect to the Ni rows. The low-energy resonance at 1.8 V is still delocalized over the whole aggregate; however, the high-energy peak at 2.2 V is present only on one side of the dimer. The asymmetry of this resonance might be induced by slightly different adsorption sites for the two dimer atoms.

In conclusion, the electronic properties of individual Au atoms and dimers on NiAl(110) have been studied with STM/STS and DFT calculations. A single, unoccupied resonance observed for Au atoms splits into a symmetric and an antisymmetric state in Au dimers. The orbital symmetry was directly visualized in spatially resolved dI/dV measurements. The peak splitting in Au dimers is strongly influenced by substrate electronic states, which reduce direct interactions at short interatomic distances and induce a slowly decaying energy splitting at larger separations. The importance of the NiAl support on the interaction between Au induced resonances has implications for a microscopic understanding of nucleation and growth processes, as well as chemical activity on solid surfaces. The experimental approach presented in this Letter enables a quantitative analysis of coupling mechanisms between adatoms on the atomic level.

This work was supported by the National Science Foundation under Grant No. 0102887. N. N. gratefully acknowledges the Deutsche Forschungsgemeinschaft for support. M. P. is thankful for support by the Swedish Research Council, the hospitality of the Institute of Surface and Interface Science at UC Irvine, and the allocation of computer resources by SNAC.

*On leave of absence from Department of Physics, Cornell University, Ithaca, NY 14853-2501.
†On sabbatical leave from Department of Applied Physics, Chalmers/Göteborg University, Göteborg, Sweden, S-41296.
‡Corresponding author.
Electronic address: wilsonho@uci.edu

[1] *Concepts in Surface Physics*, edited by M. C. Desjonqueres and D. Spanjaard (Springer, Berlin, 1993).
[2] W. R. Graham and G. Ehrlich, Phys. Rev. Lett. **31**, 1407 (1973); G. Ehrlich and K. Stolt, Annu. Rev. Phys. Chem. **31** , 603 (1980).
[3] R. Casanova and T. T. Tsong, Phys. Rev. B **22**, 5590 (1980); **24**, 3063 (1981).
[4] L. Bartels, S. Zophel, G. Meyer, E. Henze, and K. H. Rieder, Surf. Sci. **372**, L261 (1997).
[5] T. Bredow and G. Pacchioni, Surf. Sci. **426**, 106 (1999).
[6] V. Bonačic-Koutecky, J. Pittner, M. Boiron, and P. Fantucci, J. Chem. Phys. **110**, 3876 (1999).
[7] *Clusters of Atoms and Molecules*, edited by H. Haberland (Springer, Berlin, 1994).
[8] S. Fedrigo, W. Harbich, and J. Buttet, J. Chem. Phys. **99**, 5712 (1993).
[9] I. Rabin, W. Schulze, and G. Ertl, Chem. Phys. Lett. **312**, 394 (1999).
[10] T. L. Einstein, Rev. Solid State Sci. **7**, 261 (1978).
[11] A. Bogicevic *et al.*, Phys. Rev. Lett. **85**, 1910 (2000).
[12] J. Repp *et al.*, Phys. Rev. Lett. **85**, 2981 (2000).
[13] K. A. Fichthorn and M. Scheffler, Phys. Rev. Lett. **84**, 5371 (2000).
[14] H. Brune, H. Roder, C. Boragno, and K. Kern, Phys. Rev. Lett. **73**, 1955 (1994).
[15] B. C. Stipe, M. A. Rezaei, and W. Ho, Rev. Sci. Instrum. **70**, 137 (1999).
[16] G. Kresse and J. Hafner, Phys. Rev. B **47**, 558 (1993); G. Kresse and J. Furthmüller, Phys. Rev. B **54**, 11 169 (1996); G. Kresse and J. Joubert, Phys. Rev. B **59**, 1758 (1999).
[17] A 3×3 surface unit cell was used for Au atoms and dimers II and III. Dimers I and IV were modeled with a 4×2 and a 5×2 surface unit cell, respectively. The vacuum region was 14.4 Å. The surface Brillouin zone was sampled with 24 k-points. A Fermi level smearing of 0.2 eV and a 202 eV plane wave cutoff were used.
[18] J. Tersoff and D. R. Hamann, Phys. Rev. Lett. **50**, 1998 (1983).
[19] F. E. Olsson, M. Persson, N. Lorente, L. J. Lauhon, and W. Ho, J. Phys. Chem. B **106**, 8161 (2002).
[20] P. J. Feibelman, Phys. Rev. B **64**, 125403 (2001).
[21] S. C. Lui, M. H. Kang, E. J. Mele, E. W. Plummer, and D. M. Zehner, Phys. Rev. B **39**, 13 149 (1989).
[22] The tunneling gap for spectroscopy was set with $V_{\text{sample}} = 2.0$ V, $I = 0.1$ nA, resulting in a tip-sample separation of 7–8 Å.
[23] E. J. Heller, Phys. Rev. Lett. **77**, 4122 (1996).